CHARACTERIZATION OF ALUMINA BY HERTZIAN INDENTATION AND R-CURVE

S. Bouras, I. Zerizer, F. Gheldane, M.T. Bouazza, Y. Berriche

Laboratoire des matériaux avancés, Université Badji Mokhtar de Annaba B.P. 12, 23000 Annaba –Algérie.

ABSTRACT

We followed the resistance to crack propagation using the acoustic emission and the Hertzian indentation: the acoustic emission count rate decreases before the critical propagation is reached. At a critical load Pc in Hertzian indentation tests, the crack propagates at the surface as an entire circle around the ball and also in depth as a cone. The circular crack occurs progressively, step by step, in several stages according to the loading. Critical load Pc is determined by an acoustic emission peak of higher amplitude. The loads below P_c provoke weak acoustic emission translating a sub-critical crack extension related to the resistance to crack propagation. In three points bending, the increase of the stress intensity factor versus crack extension is shown clearly. In spite of the pre-existent micro-cracks presence, alumina shows a crack growth resistance that translates stable crack propagation before the fracture : the toughness increases. The bridging by grains and the crack ramification are responsible of the crack propagation resistance.

Keywords: Alumina, R-curve, resistance to crack propagation, hertzian indentation, acoustic emission.

RESUME

La propagation de fissure a été étudiée par l'émission acoustique et l'indentation hertzienne: le taux du comptage de l'émission acoustique décroît avant que la propagation critique ne soit atteinte. A une charge critique Pc, en indentation hertzienne, la fissure se propage à la surface du matériau sous forme d'un cercle autour de la bille mais aussi en profondeur sous forme d'un cône. La fissure circulaire se produit progressivement, pas à pas, en plusieurs étapes, lors du chargement. La charge critique Pc est déterminée par un pic d'émission acoustique de forte amplitude. Les charges en deçà de Pc provoquent une faible activité acoustique due à une propagation sous critique de fissure. Ceci est en accord avec une résistance à la propagation de fissure. En flexion trois points, malgré la présence des micro-fissures préexistantes, l'augmentation du facteur de l'intensité de contrainte en fonction de l'extension de la fissure est clairement montrée : l'alumine présente une résistance à l'accroissement de la fissure. Ceci traduit une propagation stable de fissure avant la rupture, alors la ténacité augmente. Le pontage par grains et la ramification de fissures sont responsables de la résistance de la propagation de la fissure.

Mots clés: Alumine, courbe-R, résistance à la propagation de fissure, indentation hertzienne, émission acoustique

INTRODUCTION

Resistance to crack propagation: R-curve effect

The ceramic brittleness is due to pre-existent micro-cracks that become unstable under the effect of a stress and leads to the fracture of the specimen [1-8]. However, alumina presents a crack growth resistance that translates stable crack propagation before the fracture. In this case, the material toughness is not constant but increases with the crack extension. It depends on the crack extension Δa from an initial crack size a. The curve representing the crack growth resistance variation R, or the stress intensity factor K_R, according to Δa is called R-curve or K_R-curve. The bridging by grains and the crack ramification are responsible for the crack propagation resistance [2].

Hertzian indentation

The hertzian indentation [9-16] consists to load specimen surface using a spherical indenter (Fig. 1). It requires the presence of an initial micro-crack that can be introduced by polishing. At a critical load P_c, this crack propagates on the surface as an entire circle around the ball and in depth as a cone [15-16]. On materials presenting a resistance to crack propagation, we observe that the circular crack occurs progressively in several stages according to the loading. Critical load P_c is determined by the highest acoustic emission peak. The acoustic emission allows to follow the resistance to crack propagation step by step until the entire circle occurs. The numbering of acoustic emission events is counted at regular intervals (rate of numbering $N/\Delta t$: number of arks by time unit)

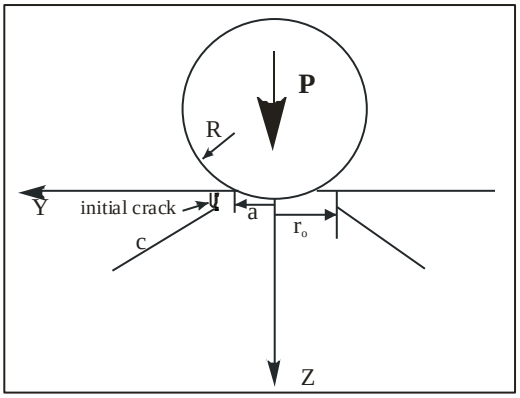

Figure 1. Schematic principle of the Hertzian indentation: a contact radius, r_o crack radius at the surface, c crack length in depth, R ball radius, P indentation load.

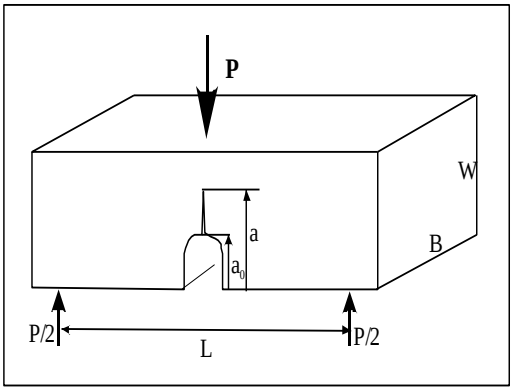

Figure 2. Schematic principle of three points bending method.

Fracture toughness tests

Tests of three points bending were carried out on SENB specimen notched with a relative depth a/w=0.5(Fig. 2). We used a universal testing machine with constant displacement speed of 5 μm/min.
The crack length at a given load was determined by an iterative method from compliance values using the following expression:

$$a_n = a_{n-1} + \frac{W - a_{n-1}}{2}\frac{C_n - C_{n-1}}{C_n} \qquad (1)$$

a_n and C_n represent respectively the crack length and the compliance of the n^{th} point of load-displacement curve. The stress intensity factor K_R was calculated in different points of the curve using the relation:

$$K_R = \frac{3PL}{2BW^2} Y(a/W)\sqrt{a} \qquad (2)$$

with

P : applied load;
a : crack length;
Y(a/W) : shape factor [20]
L : span.
B and W the width and the height of the sample

Acoustic emission

Acoustic emission designates all manifestation of an acoustic wave whose source is within a material undergoing a structural modification in presence of a mechanical solicitation. The method is highly sensitive and a sensor, even distant on the piece, detects the event source. Therefore it is not necessary to localize the source in order to detect it.

The interest of the acoustic emission is to obtain data on emissive events and to correlate them to mechanisms responsible for their generation. The used frequencies are between 50 and 400 KHz. The sensor delivers an electric signal whose amplitude is about 10 μV, and which is amplified from 50 to 100 dB and then treated. The signal (event) contains informations concerning the phenomenon source. After amplification, the signal passes by a counter that gives the number, as often as the signal passes over a constant threshold V*: it is the numbering of arks.
The numbering can be cumulative (cumulated numbering N): there is an addition of one unit to the time when the signal passes the threshold, or at regular intervals (rate of numbering N/Δt: number of arks by unit of time).
The delivered tension V(t) at the instant t is given by the expression:

$$V(t) = V_o\, e^{-\gamma t} \mathrm{Sin}(\omega t) \qquad (3)$$

Where

V_o : initial amplitude of the signal.
γ : constant of damping time.
ω : signal frequency.

The number of arks is given by the relation:

$$N = \frac{t^*}{2\pi/\omega} = \frac{\omega}{2\pi\gamma} Log\frac{V_o}{V^*} \qquad (4)$$

With

$$V^* = V_o e^{-\gamma t^*}$$

$$t^* = \frac{1}{\gamma} Log\frac{V_0}{V^*}$$

SAMPLE DESCRIPTION

The studied material was processed using a 99,7 % alumina powder pure and sintered at 1500 °C. The grain size is between 5 and 15 µm, as it can be shown in figure 3.

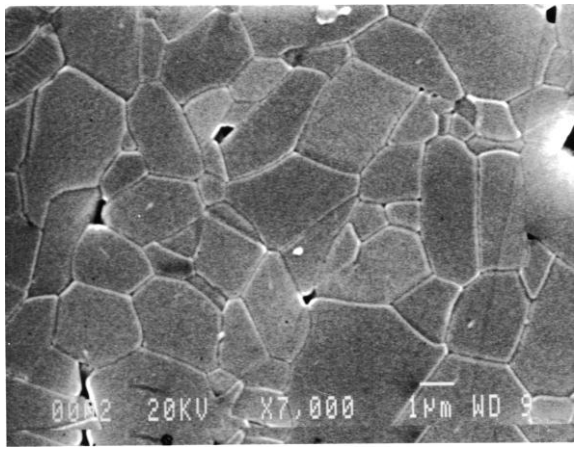

Figure 3. Microstructure of alumina.

RESULTS

Hertzian indentation

In hertzian indentation tests, the used monotonous loading leads to the progressively growth of circular cracks (fig. 4a,b) until the formation of a complete circle.

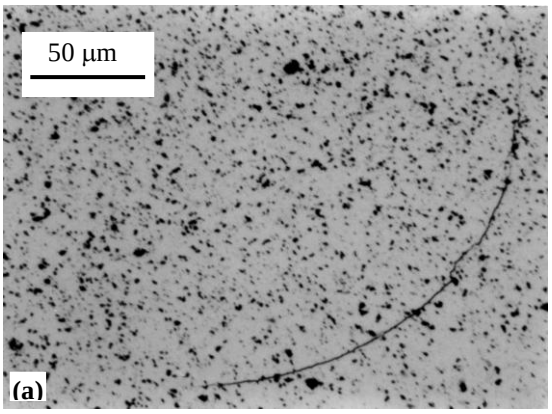

Figure 4,a. Circular cracks: P = 300 N,
Ball radius = 4 mm.

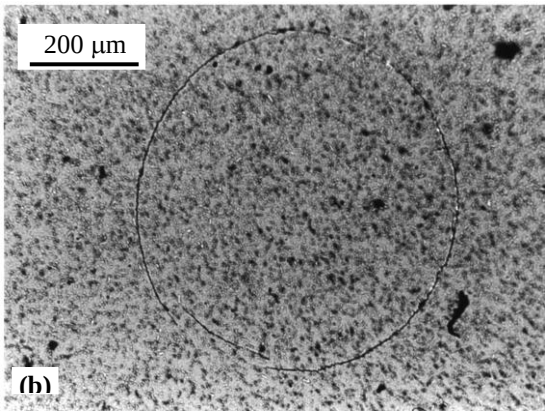

Figure 4,b. Circular cracks: P = 1000 N,
Ball radius = 4 mm.

Figure 5 shows the result of loading followed by an unloading, and the recorded acoustic emission. The complete circle occurred at the fracture critical load P_c = 900 N identified by the peak of the highest amplitude. The loads below P_c provoke weak acoustic emissions translating a sub-critical crack propagation correlated to the resistance to crack propagation.

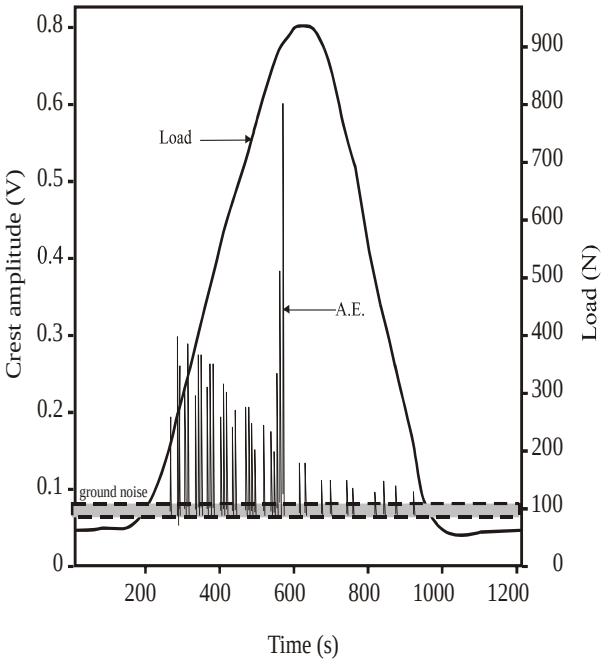

Figure 5. Acoustic emission and loading.

Figures 6a and 6b show that the arks numbering rate decreases first. That means that every time interval contains less acoustic events than the previous interval. And it translates a resistance to cracks propagation. Close to the critical load, very fast growth of the arks numbering rate is obtained.

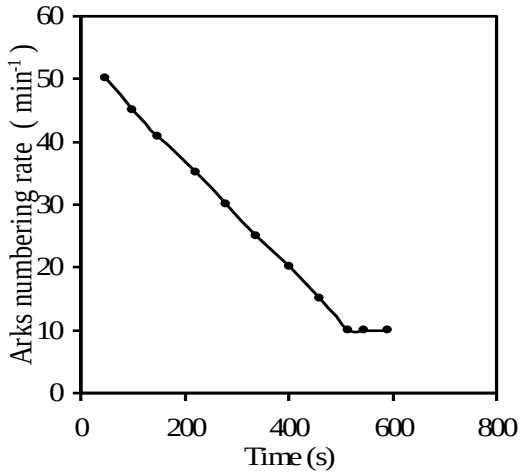

Figure 6a. Arks numbering rate.

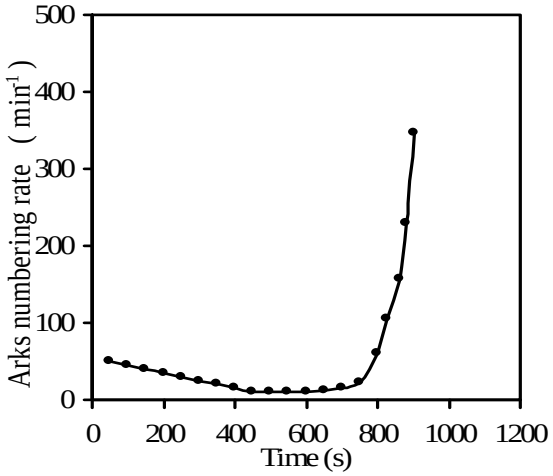

Figure 6b. Arks numbering rate until a load close to the fracture.

R-curve effect

Tests carried out by the three points bending show that K_R increases slowly to a maximal value 2.9 MPa√m (Fig. 7). This R-curve effect is due to the presence of resistance crack propagation provoked by a grain bridging or a crack ramification (Fig. 8 and 9). When the crack opening increases, the resistance crack becomes weak and we obtain a flat R-curve that decreases when the rupture of the specimen starts.

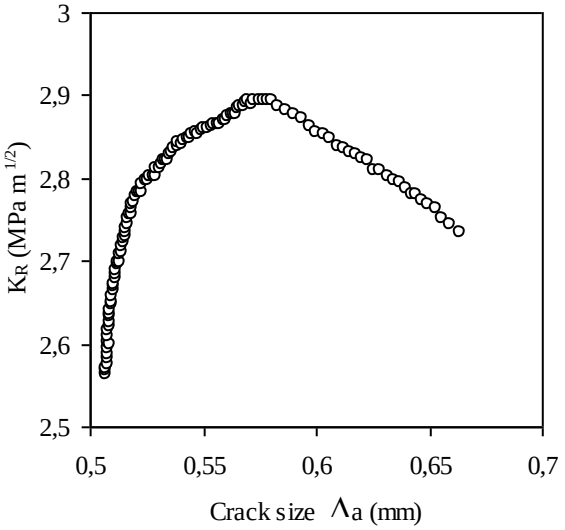

Figure 7. R-curve effect

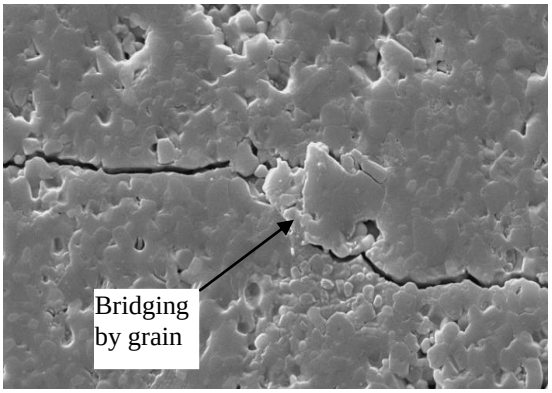

Figure 8. Photo of microstructure showing crack bridging site on the crack path

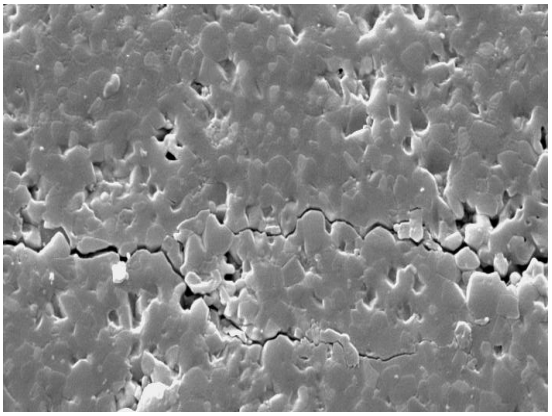

Figure 9. Photo of microstructure showing crack ramification

CONCLUSION

The resistance to the crack propagation was studied on alumina by the hertzian indentation using the acoustic emission and by the three points bending method. The decrease of the rate of the arks numbering variations obtained by acoustic emission indicates the resistance crack propagation for loads less than the critical load provoking the fracture. The fracture toughness tests showed an R-curve effect. There is a good correlation between the two methods: hertzian indentation and fracture toughness tests.

REFERENCES

[1] A.G. Evans, K.T. Faber, *"Crack Growth Resistance of Microcracking Brittle Materials", J. Am. Ceram. Soc*., Vol. 67, n°4, (1984), pp. 255-260

[2] M.V. Swain, *"R-curve Behaviour in a Polycrystalline Alumina Material", J. Mater. Sci. Letters,* Vol. 5, n°4, (1986), pp. 1313-1315

[3] B.J. Pletka, S. M. Wiederhorn *"A Comparison of Failure Predictions by Strength and Fracture Mechanics Techniques", J. Mater. Sci*., Vol. 17, (1982), pp. 1247-1268

[4] A. Okada, N. Hirosaki, *"Subcritical Crack Growth in Sintered Silicon Nitride Exhibiting a Rising R-curve", J. Am. Ceram. Soc*., Vol. 73, n°7, (1990), pp. 2095-2096

[5] B.R. Lawn, *"Fracture of Brittle Solids", Cambridge University Press*, Ch. 8 (1993).

[6] R. J. Charles, *"Dissolution Behavior of Macro Porous Glass", J. Am. Ceram. Soc*., Vol. 47, (1964), pp. 154-155

[7] JR. J. B. Wachtman. *"Highlights of Progress in the Science of Fracture of Ceramics and Glass", J. Am. Ceram. Soc*.,. Vol. 57, n°12, (1974), pp. 509-519

[8] F. F. Lange, *"In Deformation of Ceramic Materials", Pensylvania State University, Plenum Press* (1975) pp. 361-381

[9] H. Hertz, *"On the Contact of Elastic Solids", Zeitschrift für die Reine und Angewandte Mathematik, vol.9,2* (1881), pp.156-171

[10]F.C. Frank, B.R. Lawn,*"On the Theory of Hertzian Fracture", Proc. R. Soc.,* A299 (1967) pp., 291-306

[11]R. Warren, *"Measurements of the fracture properties of brittle solids by hertzian indentation", Acta. Met., Vol.26,* (1978) pp.,1759-1769

[12]R. Mouginot, and D. Maugis, *"Fracture Indentation Beneath Flat and Spherical Punches", J. Mater. Sci.,* Vol.20, (1985), pp. 4354-4376

[13]B.R. Lawn, *"Indentation of Ceramics wit, Spheres: A Century after Hertz", J. Am. Ceram. Soc.,* Vol 81, (1998), pp 1977–1994

[14]B.R. Lawn, T.R. Wilshaw ,*"Review-Indentation Fracture: Principles and Applications", J. Mater.Sci. Vol.10,* n° 6, (1975), pp.1049-1081

[15]S. Bouras, and B. Bouzabata, "Study of Hertzian Indentation on a Transparent Vitroceramic and on an Alumina", *Mat. Che. Phy*.,Vol.N°43, (1996), pp.127-134

[16]S. Bouras, "Etude par Emission de l'Indentation Hertzienne et de l'Indentation Vickers sur une Vitro-céramique et sur des Alumines", Thèse de Doctorat d'Etat, INSA de Lyon, (1993), p.186

[17]J. E. Srawley*", "Wide Range Stress Intensity Factor Expressions of ASTM E399.Standard Fracture Toughness Specimens", Int. J. Fract*., Vol. 12, n°3, (1976), pp. 475-476